# Solvation in Octanol: Parametrization of the Continuum MST Model

**CARLES CURUTCHET,[1] MODESTO OROZCO,[2] F. JAVIER LUQUE[1]**

[1]*Departament de Fisicoquímica, Facultat de Farmácia, Universitat de Barcelona, Avgda, Diagonal s/n, Barcelona 08028, Spain*

[2]*Departament de Bioquímica i Biologia Molecular, Facultat de Química, Universitat de Barcelona, c/Martí Franqués 1, 08028 Barcelona, Spain*

*Received 2 January 2001; accepted 2 March 2001*
*Published online 05 June 2001*

**ABSTRACT:** This study reports the parametrization of the HF/6-31G(d) version of the MST continuum model for *n*-octanol. Following our previous studies related to the MST parametrization for water, chloroform, and carbon tetrachloride, a detailed exploration of the definition of the solute/solvent interface has been performed. To this end, we have exploited the results obtained from free energy calculations coupled to Monte Carlo simulations, and those derived from the QM/MM analysis of solvent-induced dipoles for selected solutes. The atomic hardness parameters have been determined by fitting to the experimental free energies of solvation in octanol. The final MST model is able to reproduce the experimental free energy of solvation for 62 compounds and the octanol/water partition coefficient ($\log P_{ow}$) for 75 compounds with a root-mean-square deviation of 0.6 kcal/mol and 0.4 (in units of $\log P$), respectively. The model has been further verified by calculating the octanol/water partition coefficient for a set of 27 drugs, which were not considered in the parametrization set. A good agreement is found between predicted and experimental values of $\log P_{o/w}$, as noted in a root-mean-square deviation of 0.75 units of $\log P$. © 2001 John Wiley & Sons, Inc. J Comput Chem 22: 1180–1193, 2001

**Keywords:** octanol; continuum MST model

*Correspondence to:* F. J. Luque; e-mail: javier@far1.far.ub.es

This article includes Supplementary Material available from the authors upon request or via the Internet at ftp.wiley.com/public/journals/jcc/suppmat/22/11 or http://www.interscience.wiley.com/jpages/0192-8651/suppmat/v22.1180.html

Contract/grant sponsor: the Dirección General de Investigación Científica y Técnica; contract/grant numbers: PB98-1222 and PM99-0046

## Introduction

Many diverse biochemical, pharmacological, and toxicological processes are related to the differential solubility of solutes in aqueous and nonaqueous (organic) environments.[1–4] The understanding of the nature of solute–solvent interactions in aqueous and organic environments is thus crucial for the determination of the biological profile of chemical compounds. The hydrophobicity of a molecule can be quantified by its partition coefficient between water and an organic phase. Numerous organic solvents have been used, such as oils, chloroform, or alkanes.[5–9] However, *n*-octanol is clearly the most popular organic solvent for the study of hydrophobic properties in biological and pharmacological systems. Thus, in the sixties Hansch and Fujita[10] introduced the logarithm of the partition coefficient between octanol and water ($\log P_{ow}$) as a measure of the hydrophobicity of molecules, and this parameter continues to be the one most used in pharmacological studies.

The first semiempirical methods for the approximation of $\log P_{ow}$ were based on the sum of fragmental contributions.[11–13] Nowadays, many procedures relying on additivity schemes of group/atom-based partition contributions have been reported and implemented in several computer programs (see refs. 14 and 15 for a critical comparison of different procedures). Besides fragment additivity schemes, other semiempirical procedures rely on empirical quantitative structure–property relationships that relate the partition coefficient to other calculated molecular properties.[16–18] These methods are extensively used for the fast calculation of $\log P_{ow}$ in quantitative structure relationship studies (QSAR) in drug design projects.

From a microscopic physico-chemical point of view, *n*-octanol has a complex behavior owing to its amphipathic nature. Thus, it has a primarily lipophilic nature related to the lengthy alkyl side chain, but the presence of the polar head group enables the formation of hydrogen-bonding interactions. Overall, this solvent is relatively hydrophilic, as reflected in a dielectric constant of around 10 at 298 K[19] and the high content of water in water-saturated octanol (the mol fraction of water is 0.263 at 298 K).[20] This amphipathic nature gives *n*-octanol characteristics similar to those of lipids in biological membranes, thus giving support to the application of $\log P_{ow}$ as an indicator of hydrophobicity in biomolecular systems.

Theoretical computational techniques[21–26] have proven to be very powerful for understanding solute–solvent interactions in different solvents, and also for determining octanol/water partition coefficients. Molecular dynamics simulations have been conducted to explore the structural, thermodynamic, and dielectric properties of *n*-octanol and its water-saturated solution.[27, 28] Free energy perturbation studies have been performed to examine the structure and dynamics of small organic solutes in hydrated 1-octanol.[27, 29–31] Recently, statistical mechanics simulations have been used in the framework of linear response theory to derive empirical relationships for estimating $\log P_{ow}$ values.[32, 33] Besides discrete simulation techniques, alternative approaches have been developed in the framework of continuum methods.[21–23] In this respect, a critical discussion of different contributions to the computation of solvent transfer processes has been reported in the framework of the PCM model.[34] Very detailed parametrizations of the SMx models for determining the free energies of solvation in octanol, as well as a large number of solvents, have been reported by Cramer and Truhlar.[35–38] Furthermore, they have elaborated a specific parametrization for the fast prediction of partition coefficients.[39] The calculation of partition coefficients has also been examined in the COSMO model.[40, 41] Finally, the parametrization of a classical version of the GB/SA continuum model has been reported,[42] and its accuracy for predicting $\log P_{ow}$ values has been recently summarized by comparison with free energy calculations.[31]

In this study we report the parametrization of the HF/6-31G(d) version of the MST continuum model[43] for calculating free energies of solvation in *n*-octanol and for predicting octanol/water partition coefficients. Several reasons justify our effort. First, we are interested in methods able to treat chemical interactions in different solvents of chemical and biochemical importance. Second, the evaluation of free energies of solvation in octanol is a challenging test for any continuum model owing to the amphipathic nature of this solvent. Finally, the evaluation of $\log P_{ow}$ values using empirical procedures, though much less expensive, often fails due to (1) the occurrence of chemical processes (tautomerism, conformational equilibrium, dimerization, etc; see for instance, refs. 45, 46, and 47; (2) intrinsic limitations of the additive nature of fragment contributions; or (3) the lack of suitable parameters for new chemical groups. The parametrization of quantum mechanical continuum models can, therefore, be valuable for the study of chemical phenom-

ena in octanol, as well as to examine the transferability of fragment partition contributions.[48–50] Finally, this study also reports a reparametrization of our previous MST versions for water,[51] chloroform,[52] and carbon tetrachloride,[53] which allows a more accurate calculation of solvation free energies in all these solvents.

## Methods

### THE MST METHOD

To describe the development of the MST parametrization for octanol, we first briefly outline the main features of the MST method. The MST model relies on the continuum model (known as polarizable continuum model) originally developed by Miertus, Scrocco, and Tomasi.[23, 54, 55] The free energy of solvation in the MST model is expressed as the sum of three contributions [eq. (1)]: cavitation ($\Delta G_{cav}$), van der Waals ($\Delta G_{vW}$), and electrostatic ($G_{ele}$).

$$\Delta G_{sol} = \Delta G_{ele} + \Delta G_{cav} + \Delta G_{vW} \quad (1)$$

The electrostatic term is the difference in the work spent in charging up the solute in the bulk solvent compared to a vacuum. This component is determined treating the solvent as a continuous polarizable medium, which responds to the solute charge distribution so as to generate a reaction field. This reaction field is introduced as a perturbation operator, $V_R$, into the Schrödinger equation [eq. (2)], so that the solute and solvent polarization are determined self-consistently. The perturbation operator itself is expressed in terms of a set of imaginary charges spread over the solute cavity [eq. (3)], which are obtained by solving the Laplace equation with suitable boundary conditions [eq. (4)]. In eq. (3), $M$ is the total number of surface elements, $j$, into which the solute/solvent boundary is divided, and $\{q_j\}$ is the set of charges (located at $r_j$) that represents the solvent response. In eq. (4), $V_T$ is the total electrostatic potential, which includes both solute and solvent contributions, $n$ is the unit vector normal to the surface element $j$, $S_j$ is the area of the surface element $j$, and $\varepsilon$ is the solvent dielectric constant. Finally, it is worth noting that both the self-polarization of the charges spread on the cavity surface and charge normalization[54, 55] are explicitly accounted for in the MST method.

$$\left(H^\circ + \frac{1}{2}V_R\right)\Psi = E\Psi \quad (2)$$

$$V_R = \sum_{j=1}^{M} \frac{q_i}{|r_i - r|} \quad (3)$$

$$q_j = -\frac{\varepsilon - 1}{4\pi\varepsilon} S_j \left(\frac{\partial V_T}{\partial n}\right)_j \quad (4)$$

Solving the nonlinear Schrödinger equation [eq. (2)] provides the electrostatic contribution to $\Delta G_{sol}$, as noted in eq. (5), where the index "sol" means that the perturbation operator is adapted to the fully relaxed charge distribution of the solute in solution, and the index "0" stands for the gas phase environment.

$$\Delta G_{ele} \langle \Psi^{sol} | H^\circ + \tfrac{1}{2} V^{sol} | \Psi^{sol} \rangle - \langle \Psi^\circ | H^\circ | \Psi^\circ \rangle \quad (5)$$

The free energy of cavitation accounts for the work necessary to generate a cavity large enough to accommodate the solute in the bulk solvent. This term is computed following Pierotti's scaled particle theory[56] adapted to molecular shaped cavities according to the procedure proposed by Claverie.[57] Accordingly, the free energy of cavitation of atom $i$ ($\Delta G_{C\text{-}P,i}$) is determined weighting the cavitation free energy of the isolated atom in Pierotti's formalism ($\Delta G_{P,i}$) by the ratio between its contribution ($S_i$) to the solvent-exposed surface and the total solvent-exposed surface ($S_T$) of the molecule [eq. (6)].

$$\Delta G_{cav} = \sum_{i=1}^{N} \Delta G_{C\text{-}P,i} = \sum_{i=1}^{N} \frac{S_i}{S_T} \Delta G_{P,i} \quad (6)$$

The van der Waals component represents the contribution arising from dispersion–repulsion interactions between solute and solvent molecules. This term is determined using a linear relationship between the van der Waals free energy of a given atom, $i$, ($\Delta G_{vW,i}$) and its solvent-exposed surface, as shown in eq. (7), where $\xi_i$ is an atomic surface tension. The values of $\xi_i$ are typically determined by fitting the experimental free energies of solvation or the partition coefficients for a training set of molecules that contain prototypical functional groups.

$$\Delta G_{vW} = \sum_{i=1}^{N} \Delta G_{vW,i} = \sum_{i=1}^{N} \xi_i S_i \quad (7)$$

A dual cavity strategy has recently been introduced in the parametrized MST model.[58] This strategy defines different solute/solvent interfaces for the electrostatic ($\Delta G_{ele}$) and nonelectrostatic ($\Delta G_{cav}$, $\Delta G_{vW}$) components of the free energy of solvation. Thus, the latter contributions are determined by using a van der Waals surface built up from suitable van der Waals radii for the atoms,[19] while the electrostatic term is computed using the solvent-exposed surface defined upon an appropriate scaling of the atomic radii. This scaling factor is an adjustable parameter for a given solvent,

and it adopts a value of 1.25, 1.60, and 1.80 in the current MST-HF/6-31G(d) parametrizations for water,[51] chloroform,[52] and carbon tetrachloride,[53] respectively. The GEPOL procedure[59] is used to determine the solute/solvent interface for both the electrostatic and nonelectrostatic terms. No explicit term is considered to account for hydrogen bonding effects, although this has been done in COSMO-RS.[40]

## MONTE CARLO SIMULATIONS

Monte Carlo (MC) calculations were performed to help us in determining the best solute/solvent interface for the electrostatic component of the free energy of solvation. For this purpose, MC–free energy perturbation (FEP) calculations were performed to estimate the magnitude of the electrostatic free energy of solvation from the work necessary to annihilate the solute charges in solution. Furthermore, MC simulations were used to generate snapshots representative of the distribution of octanol molecules around a given solute. These configurations were used to compute solvent-induced shifts in the solute dipole. These two calculations help us to determine the best scaling factor that should be used to define the electrostatic boundary between solute and solvent (see above).

MC simulations were carried out at the NPT ensemble (1 atm; 298 K) using preferential sampling and periodic boundary conditions. A single solute was immersed in a cubic box containing around 270 octanol molecules (depending on the size of the solute). The parameters for octanol were taken from the values reported by DeBolt and Kollman[27] and adapted to the OPLS[60, 61] formalism. Test MC simulations were performed to verify that physical properties (heat of vaporization, density) were reproduced correctly. Electrostatic potential-derived atomic charges[62–65] computed at the RHF/6-31G(d)[66] level were used with standard OPLS Lennard-Jones parameters for the solutes. MC simulations were run considering 6 million configurations for equilibration and 6 million configurations for data collection. A residue-based nonbonded cutoff of 9 Å was used to evaluate intermolecular interactions. The internal geometry of the solute was kept fixed in simulations. Rotations and translations of the solute and solvent molecules were adjusted to give 40–50% acceptance.

Fifty snapshots uniformly taken from the MC simulation were used to compute the influence of the octanol molecules on the dipole moment of the solvent. To this end, RHF/6-31G(d) wave functions were computed for the series of solutes immersed in the solvent atomic charge cloud. From these calculations (and the reference gas-phase calculation) the magnitude of the gas phase → octanol-induced dipole moment was averaged.

MC–FEP simulations were performed in 21 windows using the double-wide sampling technique. For each window the system was equilibrated over at least 6 million configurations, and the average was done for 6 million configurations. The starting structure in MC–FEP simulations was taken from the last snapshot obtained in the MC simulation of the solute in octanol mentioned above. The technical conditions used in the MC–FEP simulations were identical to those mentioned above for MC simulations. In all cases the hysteresis and the standard deviations were small, which lends confidence to the protocol of the simulation.

## PARAMETRIZATION DATA SET

A particular problem in the parametrization of SCRF models for octanol is the high content of water in water-saturated octanol solutions. In fact, there are limited data available for the free energy of solvation in anhydrous octanol. Fortunately, there is in general very little difference in the free energies of solvation determined in neat and water-saturated octanol,[20, 67–70] which justifies the use of free energies of solvation derived from hydrated octanol. Typically, this difference amounts to 0.2–0.4 kcal/mol. Therefore, for our purposes here we use free energies of solvation derived from hydrated octanol. A total of 58 compounds, representative of diverse functional groups has been used to define a database for parametrization of the van der Waals component of the free energy of solvation in octanol. In addition, the parameters have been refined from the comparison between experimental and calculated $\log P_{o/w}$ values for 75 compounds. These values have been taken from the data compiled by Hansch et al.[71] When more than one $\log P_{o/w}$ value is reported, the value recommended in ref. 71 has been used in the parametrization. With regard to our previous parametrizations in water,[51] chloroform,[52] and carbon tetrachloride,[53] a larger number of compounds have been used in the current reparametrization of the MST model for these solvents (69, 54 and 47 molecules for water, chloroform, and carbon tetrachloride, respectively).

## COMPUTATIONAL DETAILS

MST calculations were performed using a locally modified version of Monstergauss.[72] MC simula-

tions were carried out with the BOSS4.2 program.[61] Gas-phase geometry optimization of the molecules was performed with Gaussian 94.[73]

## Results and Discussion

### SELECTION OF THE ELECTROSTATIC SOLUTE/SOLVENT INTERFACE

The magnitude of the electrostatic component of the free energy of solvation in SCRF methods largely depends on the size of the cavity that defines the electrostatic solute/solvent boundary. Such a dependence is extremely important in polar solvents like water,[51, 74, 75] but it is still sensitive in low dielectric solvents.[52, 53] Thus, the determination of the cavity size is a delicate step in the development of the HF/6-31G(d) parametrization of the MST model for octanol. Test calculations showed us that the use of an incorrect cavity (for instance, that used in water) can still lead to a suitable free energy of solvation in octanol after the parametrization of the steric term. However, the weights of the different terms are unphysically biased if an unsuitable cavity is used in the calculation of $\Delta G_{ele}$.

In line with our previous MST parametrizations, the strategy adopted here is twofold (see Methods). First, to estimate the electrostatic free energy ($\Delta G_{ele}$) from MC–FEP simulations where the solute charges are annihilated. Second, to determine the solvent-induced dipole moment ($\Delta\mu$) of the solute from QM calculations of representative configurations of the octanol distribution around the solute. Comparison of the $\Delta G_{ele}$ and $\Delta\mu$ values determined from both classical MC–FEP and QM(RHF/6-31G(d)) calculations with the corresponding MST results is exploited to determine the best electrostatic solute/solvent interface.

To this end, we selected a series of small, neutral polar solutes, which possess prototypical functional groups: methanol, propanol, *n*-octanol, phenol, acetone, acetic acid, methyl ethanoate, acetamide, pyridine, and nitroethane. For each solute a series of MST calculations was performed by changing systematically the factor ($\kappa$) that multiplies the van der Waals radii between values of 1.25 and 1.8, which are the scaling factors parametrized for water[51] and carbon tetrachloride,[53] respectively. A value of 9.93 was taken for the dielectric permittivity of octanol at 298 K.[19] The electrostatic free energies determined at every scaling factor were then compared with the $\Delta G_{ele}$ values estimated from MC–FEP simulations. Such a comparison is shown in Figure 1,

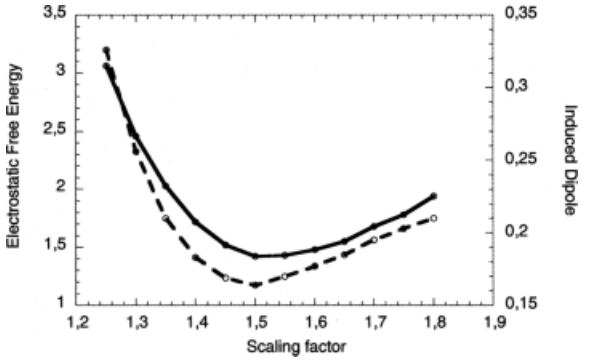


**FIGURE 1.** Representation of the change in the root-mean-square (rms) deviation (solid line) between the electrostatic component of the free energy of solvation (kcal/mol) computed from MC–FEP simulations and MST calculations, and (dashed line) between the average induced dipoles computed at the RHF/6-31G(d) level for solute/octanol configurations selected from MC simulations and at the MST level, as a function of the factor that scales the location of the solute/solvent interface for the electrostatic free energy in the MST model.

which shows that the root-mean-square (rms) deviation between MST and MC–FEP results is minimum when $\kappa$ is comprised between 1.45 and 1.6. To further investigate the definition of the solute/solvent interface, we examined the polarization of the solute upon solvation in octanol, as this property depends on the cavity size. The rms deviation between the induced dipoles ($\Delta\mu$) values computed at the RHF/6-31G(d) level (averaged for 50 configurations of the solute in octanol; see Methods) and the values obtained from the wave function derived using the MST methods for different cavities is also shown in Figure 1. The rms deviation between QM/MM and SCRF values is minimum in the interval comprised between $\kappa = 1.45$ and $\kappa = 1.55$.

The preceding results indicate that the van der Waals radii must be scaled by a factor close to 1.5 to built up the solute/octanol electrostatic interface in the MST framework. Certainly, the reliability of the MC–FEP $\Delta G_{eler}$ values and the RHF/6-31G(d) $\Delta\mu$ results (determined from selected MC configurations) is modulated by the balance between atomic point charges and van der Waals parameters in the force field and the neglect of polarization effects in MC calculations. Owing to these limitations, the definition of $\kappa$ for octanol admits some flexibility. In fact, no significant differences were observed between the statistical parameters of the models parametrized using $\kappa = 1.45$, $\kappa = 1.50$ or $\kappa = 1.55$ (see below). All of them, indeed, provided comparable changes in electrostatic properties (atomic charges

and dipole moments) upon solvation. However, the use of a scaling factor similar to that used for water ($\kappa = 1.25$) leads to $\Delta G_{ele}$ and $\Delta\mu$ values around 200 and 160% larger (in absolute value) than the corresponding values determined using $\kappa = 1.50$. Finally, we also examined the possibility of using different scaling factors for polar ($\kappa = 1.25$) and apolar ($\kappa = 1.50$) atoms or functional groups. This procedure introduces some arbitrariness in the definition of polar/apolar units within a molecule, and both $\Delta G_{ele}$ and $\Delta\mu$ values were still overestimated, especially for the most polar molecules, so we did not pursue this further.

In summary, the preceding analysis prompted us to build up the electrostatic solute/solvent interface in octanol using a scaling factor of 1.5. This empirically adjusted value for octanol is reasonable, as it is a compromise between the values parametrized for water ($\kappa = 1.25$) and for chloroform ($\kappa = 1.60$). However, note that the transferability of these scaling factors, which have been adjusted for MST calculations, to other SCRF formalisms is not assured. Indeed, the suitability of their application to continuum calculations based on DFT or *ab initio* correlated methods should also be examined.

## PARAMETRIZATION OF THE NONELECTROSTATIC TERM

Calculation of the cavitation free energy within the Pierotti–Claverie formalism [eq. (6)] requires knowledge of the number density, which can be derived from molecular weight and mass density, and the molecular diameter of the solvent. Mass density was taken from data in the literature at 298 K:[19] 0.826 g cm$^{-3}$. The assignment of the molecular diameter is more difficult, owing to the flexible structure of *n*-octanol. However, we adopted a value of 6.84 Å, which was determined from the analysis of Xe solubility data in octanol (measured as a function of temperature in the range 283–323 K) with the scaled-particle theory.[76] A similar value (6.62 Å) was previously found from solubility data of various gases in octanol in the temperature range 293–313 K.[77]

The van der Waals component is determined from a linear relationship with the atomic van der Waals surface [eq. (7)], which is built up from the atomic radii given in Table I. The atomic van der Waals hardness of atom type $i$ ($\xi_i$) is obtained from multiple linear regression to the experimental free energies of solvation [eq. (8)]. We have followed our main fitting strategy: i.e., to obtain the best possible fitting to experimental data, but introducing the smallest number of variables in the fitting. Compared to our previous MST models for water, chloroform, and carbon tetrachloride, there are some differences in the present parametrization. First, a larger number of compounds have been included in the parametrization data set (see Methods). Second, the number of atom types considered for the van der Waals contribution has been also enlarged. Third, in water different radii were defined for N, O, and S depending on their chemical environment. Finally, a correction term was included for nitrile derivatives in all solvents. The optimized atomic van der Waals parameters of the MST model are given in Table II.

**TABLE I.**
**Atomic van der Waals Radius (Å) Used in MST Calculations in Water, Octanol, Chloroform, and Carbon Tetrachloride.**

| | | | | | |
|---|---|---|---|---|---|
| General | | | | | |
| H | 1.2 (0.9)[a] | | | | |
| C | 1.5 | | | | |
| N | 1.5 | | | | |
| O | 1.4 | | | | |
| F | 1.35 | | | | |
| S | 1.75 | | | | |
| Cl | 1.8 | | | | |
| Specific for water | | | | | |
| N | in —N 1.4 | O | in —OH 1.45 | S | in —SH 1.85 |
| | in —$NH_2$ 1.55 | | | | |

[a] The radius for a hydrogen atom bound to heteroatom is given in parenthesis.

$$\Delta G_{vW} = \text{minimum}\{\Delta G_{exp} - \Delta G_{ele} - \Delta G_{cav}\} \quad (8)$$

Regarding the van der Waals hardness, because hydrogen atoms bound to heteroatom (X) typically contribute very little to the molecular surface, it was found more convenient to assign the same van der Waals parameter to both the heteroatom and the hydrogen (X—H) atoms. Indeed, a more detailed differentiation of carbon atoms is made (see Table II). This was necessary to describe the effect of increasing the number of methylene units for compounds possessing a common functional group, but differing in the length of the alkyl side chain. These modifications suffice to reproduce with good accuracy the free energies of solvation in octanol, chloroform, and carbon tetrachloride. The only exception were nitrile compounds, because MST–HF/6-31G(d) calculations revealed a systematic tendency to overestimate (in absolute value) the free energy of solvation irrespective of the solvent, which in turn, originates from an exaggeration of the electrostatic free energy component, typical of

**TABLE II.**
**Optimized Parameters[a] for MST Calculations in Water, Octanol, Chloroform, and Carbon Tetrachloride.**

| Parameters | Water | *n*-Octanol | Chloroform | Carbon Tetrachloride |
|---|---|---|---|---|
| $\kappa$ | 1.25 | 1.50 | 1.60 | 1.80 |
| $\xi$ | | | | |
| C | −0.1838 | −0.2784 | −0.1914 | −0.2182 |
| CH | −0.1272 | −0.1871 | −0.1527 | −0.1488 |
| $CH_2$ | −0.1334 | −0.1952 | −0.1490 | −0.1435 |
| $CH_3$ | −0.1250 | −0.1794 | −0.1426 | −0.1339 |
| N | −0.1258 | −0.2315 | −0.2244 | −0.2198 |
| NH | −0.1336 | −0.2536 | −0.1687 | −0.1699 |
| O | −0.0205 | −0.1413 | −0.1440 | −0.1394 |
| OH | −0.1400 | −0.2262 | −0.1586 | −0.1722 |
| F | −0.0627 | −0.1292 | −0.0832 | −0.0538 |
| S | −0.1178 | −0.1974 | −0.1661 | −0.1178 |
| SH | −0.0848 | −0.1768 | −0.1836 | — |
| Cl | −0.1088 | −0.1637 | −0.1264 | −0.1231 |
| $\Delta G_{corr}$(CN) | 3.8 | 3.8 | 2.6 | 2.7 |

[a] $\kappa$: scaling factor for the solute/solvent electrostatic interface; $\xi$: atomic van der Waals hardness (kcal mol$^{-1}$ Å$^{-2}$); $\Delta G_{corr}$(CN): correction term (kcal mol$^{-1}$) for the systematic deviation observed in nitrile derivatives (see text for more details).

a RHF representation. Therefore, an additional term was also included to correct this systematic deviation in nitrile compounds (see Table II).

Less accurate results were obtained for the free energies of solvation in water, particularly for small, polar molecules like water or ammonia. This was expected, keeping in mind the large contribution of the electrostatic term to the free energy of hydration of neutral, polar molecules, and the large sensitivity of the electrostatic free energy to the solute cavity. In fact, several formalisms that derive atomic radii from the geometry of the molecule or the electronic charge density[77–80] have been reported in the literature. Alternatively, the atomic radii have also been optimized by calibrating solvation free energies for representative solutes.[40, 80, 81] After several tests we found more convenient to refine the atomic radius of heteroatoms, which were assigned different values depending on the number of bonded hydrogen atoms (see Table I). This procedure allows a fast introduction of chemical environments effects in the determination of solute cavities.

## SOLVATION IN *n*-OCTANOL

The statistical analysis of the free energies of solvation determined from MST–HF/6-31G(d) calculations for the series of compounds included in the parametrization data set are given in Table III. The rms deviation between theoretical and experimental free energies of solvation is 0.7, 0.6, 0.4, and 0.3 kcal/mol for solvation in water, octanol, chloroform, and carbon tetrachloride, respectively. In all cases, the mean signed deviation is close to zero, and the ratio between experimental and theoretical values is close to unity, which reveals the lack of systematic errors. Finally, the regression equation $\Delta G_{exp}$ vs. $\Delta G_{sol}$ explains more than 92% of the variance of the experimental data. Overall, there is excellent agreement between experimental and theoretical free energies of solvation in all the solvents for a large, diverse series of prototypical chemical compounds.

**TABLE III.**
**Statistical Comparison[a] between the Free Energies of Solvation Computed for the Compounds Included in the Parametrization Data Set from MST-HF/6-31G(d) Calculations and the Experimental Values in Water, Octanol, Chloroform, and Carbon Tetrachloride.**

| | | | | |
|---|---|---|---|---|
| rms | 0.7 | 0.6 | 0.4 | 0.3 |
| mue | 0.6 | 0.5 | 0.3 | 0.2 |
| mse | 0.0 | 0.1 | 0.0 | 0.0 |
| *c* | 1.00 | 0.99 | 1.00 | 1.00 |
| *r* | 0.96 | 0.96 | 0.97 | 0.99 |

[a] rms: root-mean-square deviation (kcal/mol); mue: mean unsigned deviation (kcal/mol); mse: mean signed deviation (kcal/mol); *c*: scaling coefficient in the regression equation $\Delta G_{exp} = c\Delta G_{sol}$; *r*: correlation coefficient.

The MST–HF/6-31G(d) free energies of solvation and its electrostatic and nonelectrostatic components for the compounds included in the parametrization data set are given in Table IV for solvation in octanol, and in Tables I–III of Supporting Information for solvation in water, chloroform, and carbon tetrachloride, respectively. The electrostatic contribution accounts, on average, for near 50% of the free energy of solvation of polar molecules in octanol. This value is clearly lower than the contribution of $\Delta G_{ele}$ in water, where it is the dominant term (around 130% of $\Delta G_{sol}$), but notably larger than the contribution of $\Delta G_{ele}$ in chlorofom and carbon tetrachloride, where it only accounts for near 35 and 15% of $\Delta G_{sol}$, respectively. In addition, the nonelectrostatic component is negative, as it is also found in chloroform and carbon tetrachloride, whereas it is positive in water. This indicates that the cavitation work is smaller (in absolute value) than the free energy associated with dispersion interactions between the solute and the *n*-octanol molecules. These results evidence the balance between hydrophilic and lipophilic characteristics of octanol as bulk solvent, because both electrostatic and nonelectrostatic terms have a similar contribution to the free energy of solvation of polar solutes.

The polarization of the solute can be examined from the magnitude of the solvent-induced dipole moment. Figure 2 shows that the dipole moment of polar molecules is increased, on average, by 16% upon solvation in octanol. The variation of the dipole moment in octanol is near half the change that takes places upon hydration (the dipole moment is enlarged by around 35%), and as expected, larger than the solvent-induced dipole enhancement that occurs upon solvation in chloroform (12%) and in carbon tetrachloride (6%).

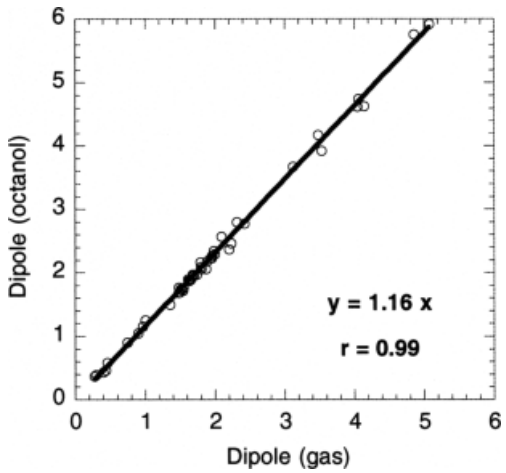


**FIGURE 2.** Representation of the dipole moment (Debyes) of neutral, polar solutes in octanol and in the gas phase. Values determined from MST–HF/6-31G(d) calculations.

The preceding results suggest that the solvation in octanol is the result of a subtle balance between electrostatic and steric contributions. This finding agrees with the analysis of the factors that govern solvation in octanol derived by using a linear-response approach in conjunction with statistical mechanics simulations.[32] SCRF results suggest then that the unique properties of *n*-octanol are derived from its being a solvent with mixed polar/apolar characteristics.

## PREDICTION OF OCTANOL/WATER PARTITION COEFFICIENTS

One of the main goals of any parametrization for octanol is the prediction of octanol/water partition coefficient. The *a priori* prediction of partition coefficients from the corresponding free energies of solvation in the two solvents is delicate owing to the error propagation. Thus, assuming a quadratic propagation of the error in the free energies of solvation and that the error is measured by the rms deviation (see Table III), the uncertainty in the partition coefficient can be estimated to be around 1.0 units of $\log P_{ow}$.

Table V gives the experimental (taken from ref. 71) octanol/water partition coefficients and the corresponding $\log P_{ow}$ values determined from MST calculations in water and in octanol. Comparison of experimental and calculated values is made in Figure 3. The regression coefficient is close to unity, and the correlation coefficient is 0.96. The largest errors ($\geq$0.7 unit of $\log P$) occur for *n*-heptanol, piperidine, nitroethane, and nitropropane. The rms deviation is 0.4 units of $\log P$, and the mean signed error is $-0.1$ units of $\log P$, which indicates the lack of systematic deviations. Similar statististical results are obtained for the subset of compounds simultaneously present in the data sets used for water and octanol (49 compounds) and for the subset of compounds used either in the data of water or octanol (26 compounds).

To further investigate the capability of the MST parametrization for predicting to octanol/water partition coefficients, we determined the $\log P_{ow}$ values for a series of heterocyclic compounds, as they are structural elements in many biologically relevant molecules. The selected compounds are shown in Table VI. The rms deviation and the mean signed signed deviation between calculated and ex-

**TABLE IV.**

**Free Energy of Solvation ($\Delta G_{sol}$) and Its Electrostatic ($\Delta G_{ele}$), Cavitation ($\Delta G_{cav}$), and van der Waals ($\Delta G_{vW}$) Components (kcal/mol) Determined from MST Calculations of Selected Compounds in *n*-octanol.**

| Compound | $\Delta G_{ele}$ | $\Delta G_{cav}$ | $\Delta G_{vW}$ | $\Delta G_{sol}$ | $\Delta G_{exp}$ |
|---|---|---|---|---|---|
| C, H | | | | | |
| Methane | −0.1 | 8.1 | −7.5 | 0.5 | 0.5 |
| Ethane | 0.0 | 12.1 | −12.7 | −0.6 | −0.6 |
| Neopentane | −0.1 | 24.0 | −25.3 | −1.4 | −1.7 |
| Cyclohexane | −0.1 | 24.2 | −27.6 | −3.4 | −3.7 |
| Hexane | −0.1 | 28.4 | −31.2 | −2.9 | −3.3 |
| Heptane | −0.1 | 32.4 | −35.8 | −3.5 | −4.1 |
| Octane | −0.1 | 36.4 | −40.4 | −4.1 | −4.6 |
| Ethylene | −0.6 | 9.9 | −11.6 | −2.2 | −0.3 |
| Methylpropene | −0.6 | 18.0 | −20.2 | −2.8 | −2.0 |
| 1-Butene | −0.5 | 18.0 | −20.1 | −2.6 | −1.9 |
| Benzene | −1.3 | 17.5 | −19.9 | −3.7 | −3.7 |
| Toluene | −1.3 | 21.5 | −24.6 | −4.4 | −4.6 |
| C, H, N | | | | | |
| Methylamine | −2.4 | 10.1 | −12.2 | −4.6 | −3.8 |
| Ethylamine | −2.4 | 14.1 | −16.8 | −5.1 | −4.1 |
| *n*-Propylamine | −2.4 | 18.2 | −21.4 | −5.7 | −4.8 |
| *n*-Butylamine | −2.4 | 22.2 | −26.1 | −6.3 | −5.4 |
| Diethylamine | −1.4 | 22.5 | −25.4 | −4.2 | −4.8 |
| Trimethylamine | −1.0 | 18.8 | −20.1 | −2.4 | −3.6 |
| Acetonitrile | −3.9 | 10.8 | −14.8 | −3.2 | −3.2 |
| Propanenitrile | −3.8 | 14.9 | −19.4 | −3.7 | −3.7 |
| Butanenitrile | −3.8 | 18.9 | −24.0 | −4.3 | −4.3 |
| Benzonitrile | −3.9 | 20.1 | −26.9 | −6.0 | −6.1 |
| Pyridine | −2.4 | 16.3 | −19.4 | −5.4 | −5.3 |
| Piperidine | −1.4 | 22.5 | −26.5 | −5.4 | −6.3 |
| C, H, O | | | | | |
| Water | −4.6 | 4.9 | −6.3 | −6.0 | −4.4 |
| Methanol | −3.0 | 9.4 | −10.7 | −4.3 | −3.9 |
| Ethanol | −2.7 | 13.4 | −15.3 | −4.6 | −4.4 |
| *n*-Propanol | −2.7 | 17.4 | −19.9 | −5.2 | −5.0 |
| *n*-Butanol | −2.7 | 21.5 | −24.6 | −5.8 | −5.7 |
| *n*-Pentanol | −2.7 | 25.5 | −29.1 | −6.3 | −6.4 |
| *n*-Hexanol | −2.8 | 29.6 | −33.8 | −7.0 | −7.1 |
| *n*-Heptanol | −2.8 | 33.6 | −38.4 | −7.5 | −7.8 |
| *n*-Octanol | −3.0 | 37.7 | −42.9 | −8.3 | −8.1 |
| Phenol | −3.4 | 18.7 | −22.6 | −7.2 | −8.7 |
| Dimethyl ether | −1.6 | 13.8 | −14.2 | −2.0 | −2.1 |
| Anisole | −2.2 | 23.1 | −25.9 | −5.0 | −5.5 |
| Tetrahydrofuran | −1.9 | 18.3 | −20.5 | −4.1 | −3.9 |
| Acetone | −3.2 | 15.7 | −16.9 | −4.4 | −3.2 |
| Benzaldehyde | −3.3 | 21.0 | −24.0 | −6.3 | −6.1 |
| Acetic acid | −4.2 | 12.8 | −14.7 | −6.1 | −6.4 |
| Propionic acid | −3.9 | 16.9 | −19.3 | −6.4 | −6.9 |
| Butiric acid | −3.9 | 20.9 | −23.9 | −6.9 | −7.6 |
| Methylethanoate | −2.8 | 17.2 | −18.3 | −3.9 | −3.5 |
| Methylbenzoate | −3.0 | 26.2 | −29.7 | −6.5 | −7.3 |

**TABLE IV.**
**(Continued)**

| Compound | $\Delta G_{ele}$ | $\Delta G_{cav}$ | $\Delta G_{vW}$ | $\Delta G_{sol}$ | $\Delta G_{exp}$ |
|---|---|---|---|---|---|
| C, H, S | | | | | |
| 1-Propanethiol | −1.6 | 18.9 | −21.2 | −4.0 | −3.5 |
| Dimethylthioether | −1.5 | 15.2 | −17.2 | −3.5 | −4.2 |
| Diethylthioether | −1.5 | 23.3 | −26.4 | −4.6 | −4.1 |
| Tiophenol | −1.9 | 20.2 | −23.8 | −5.5 | −6.0 |
| Thioanisole | −1.8 | 24.6 | −29.0 | −6.3 | −6.5 |
| Thiophene | −1.3 | 15.0 | −18.1 | −4.4 | −3.9 |
| C, H, N, O | | | | | |
| Acetamide | −6.0 | 13.5 | −16.1 | −8.6 | −8.0 |
| Nitroethane | −4.2 | 16.0 | −16.8 | −5.0 | −3.9 |
| Nitrobenzene | −3.8 | 21.0 | −23.8 | −6.6 | −6.6 |
| C, H, Halogens | | | | | |
| Tetrafluoromethane | −0.2 | 10.3 | −8.7 | 1.4 | 1.5 |
| 1,1-Difluoroethane | −1.8 | 13.2 | −12.8 | −1.3 | −1.1 |
| 2,2,2-Trifluoroethanol | −4.3 | 15.0 | −15.4 | −4.8 | −4.8 |
| Fluorobenzene | −1.4 | 18.1 | −20.4 | −3.8 | −3.9 |
| Chloroethane | −1.4 | 14.3 | −16.0 | −3.1 | −2.6 |
| Chloroform | −0.9 | 14.3 | −17.1 | −3.7 | −3.8 |
| *p*-Dichlorobenzene | −1.3 | 21.7 | −26.4 | −6.0 | −5.7 |
| Fluorotrichloromethane | −0.2 | 14.7 | −17.0 | −2.4 | −2.6 |
| Difluorodichloromethane | −0.1 | 13.3 | −14.2 | −1.1 | −1.3 |

The experimental value ($\Delta G_{exp}$) is given in the last column.

perimental $\log P_{ow}$ values are 0.6 and 0.0 units of $\log P$ (determined by excluding pyridine and thiophene, which were included in the parametrization data set). The agreement of these results with the statistical parameters mentioned above gives confidence in the ability of the MST model to reproduce accurately the partition coefficient between octanol and water of a wide variety of compounds, not considered at all in the data base used for parametrization.

As a final test of the method, we have determined the $\log P_{o/w}$ values for a series of 27 drugs, which were chosen to have little conformational flexibility. Thus, we imposed as a criteria that the drug does not possess more than four torsional degrees of freedom, and that no more than two torsional dihedrals should be contiguous along the skeletonon of the drug. The computed $\log P_{o/w}$ values are given in Table VII, which also shows the available experimental data for comparison purposes. The largest error between computed and experimental partition coefficients amounts to 1.4 units of $\log P$, corresponding to caffeine. The rms deviation between calculated and experimental $\log P_{o/w}$ values amounts to 0.75 units of $\log P$, which is slightly larger than the rms error obtained for the series of compounds included in the parametrization data set (see above). The mean signed error is −0.1 units of $\log P$, revealing the lack of any systematic deviation in the balance between the solvation in water and in octanol. Overall, keeping in mind the nature of the estimation of $\log P_{ow}$ from the free energies of hydration in the two solvents and the structural diversity of the drugs, the agreement between experimental and predicted values is satisfactory.

## Concluding Remarks

We have presented here the parametrization of the MST–HF/6-31G(d) version for solvation in octanol, and the refinement of the previous parametrizations performed for water, chloroform, and carbon tetrachloride. In agreement with our previous studies, the solute/solvent boundary has been defined from the comparison with results derived from discrete simulations. A scaling factor of 1.5 is proposed for the definition of the electrostatic

**TABLE V.**
**Calculated and Experimental *n*-Octanol/Water Partition Coefficient for the Series of Compounds Used in the Parametrization for Water and Octanol.**

| Compound | Calc. | Expt.[a] |
|---|---|---|
| C, H | | |
| Methane | 1.1 | 1.1 |
| Ethane | 1.5 | 1.8 |
| Neopentane | 3.0 | 3.1 |
| Hexane | 4.0 | 3.9 |
| Heptane | 4.6 | 4.7 |
| Octane | 5.2 | 5.2 |
| Cyclohexane | 3.7 | 3.4 |
| Ethylene | 1.2 | 1.1 |
| 2-Methylpropene | 1.9 | 2.3 |
| 1-Butene | 1.9 | 2.4 |
| Benzene | 2.3 | 2.1 |
| Toluene | 2.7 | 2.7 |
| *m*-Xylene | 3.1 | 3.2 |
| C, H, N | | |
| Methylamine | −0.1 | −0.6 |
| Ethylamine | 0.3 | −0.1 |
| Propylamine | 0.7 | 0.5 |
| Butylamine | 1.2 | 1.0 |
| Dimethylamine | 0.3 | −0.4 |
| Diethylamine | 1.2 | 0.6 |
| Trimethylamine | 0.6 | 0.2 |
| Aniline | 2.1 | 0.9 |
| Piperidine | 1.6 | 0.8 |
| Pyridine | 0.4 | 0.7 (0.6) |
| 4-Methylpyridine | 0.6 | 1.2 |
| Acetonitrile | 0.0 | −0.3 |
| Benzonitrile | 0.9 | 1.6 |
| C, H, O | | |
| Water | −0.8 | −1.4 (−1.2) |
| Methanol | −1.0 | −0.8 (−0.3; −0.5) |
| Ethanol | −0.3 | −0.3 (−0.2; −0.4) |
| *n*-Propanol | 0.1 | 0.3 |
| 2-Propanol | −0.1 | 0.1 |
| *n*-Butanol | 0.7 | 0.9 |
| *n*-Pentanol | 1.0 | 1.6 |
| *n*-Hexanol | 1.7 | 2.0 |
| *n*-Heptanol | 2.0 | 2.7 |
| *n*-Octanol | 2.4 | 3.0 |
| Phenol | 1.2 | 1.5 (0.6) |
| *o*-Methylphenol | 2.2 | 2.0 |
| *p*-Methylphenol | 1.9 | 1.9 (2.0) |
| Dimethylether | 0.6 | 0.1 |
| Diethylether | 1.3 | 0.9 |
| Anisole | 2.3 | 2.1 |
| Tetrahydrofuran | 0.7 | 0.5 |
| Benzaldehyde | 1.1 | 1.5 |
| *p*-Hydroxybelzaldehyde | 0.8 | 1.4 |
| Acetone | 0.2 | −0.2 |
| Butanone | 0.7 | 0.3 |
| Acetophenone | 1.4 | 1.6 |
| Acetic acid | −0.6 | −0.2 |
| Propionic acid | 0.0 | 0.3 |
| Butiric acid | 0.6 | 0.8 |
| Metbylacetate | 0.9 | 0.2 |
| Ethylacetate | 0.7 | 0.7 |
| Methylpropanoate | 1.4 | 0.8 |
| Methylbenzoate | 2.5 | 2.1 |
| C, H, N, O | | |
| Acetamide | −0.9 | −1.3 |
| Nitroethane | 1.1 | 0.2 |
| Nitropropane | 1.7 | 0.9 |
| Nitrobenzene | 1.6 | 1.9 |
| C, H, S | | |
| Propanethiol | 2.1 | 1.8 |
| Thiophenol | 2.9 | 2.5 |
| Diethylthioether | 2.2 | 2.0 |
| Thioanisole | 3.0 | 2.7 |
| Tiophene | 2.3 | 1.8 |
| C, H, Halogens | | |
| Fluoromethane | 0.0 | 0.5 |
| Tetrafluoromethane | 1.7 | 1.2 |
| 1,1-Difluoroethane | 0.6 | 0.8 |
| 2,2,2,-Trifluoroethane | 0.0 | 0.4 |
| Fluorobenzene | 2.2 | 2.3 |
| Chloroethane | 1.2 | 1.4 |
| Chlorobenzene | 2.8 | 2.8 |
| *p*-Dichlorobenzene | 3.4 | 3.4 |
| Difluorodichloromethane | 2.6 | 2.2 |
| Fluorotrichloromethane | 3.0 | 2.5 |

[a] When more than one $\log P_{ow}$ value is available, the value recommended by Hansch and Leo[71] is indicated, and the rest of values are given in parenthesis.

boundary in octanol. The parametrization of the van der Waals component by fitting to experimental data shows that the MST model is able to reproduce accurately the free energies of solvation in octanol for a variety of organic neutral, polar compounds. Moreover, the octanol/water partition coefficients predicted from the free energies of solvation in octanol and water reproduce satisfactorily the experimental $\log P_{ow}$ values for a wide range of compounds including many real drugs.

Compared to simpler QSAR-based methods for prediction of octanol/water partition coefficients, the MST–HF/6-31G(d) model is clearly much more

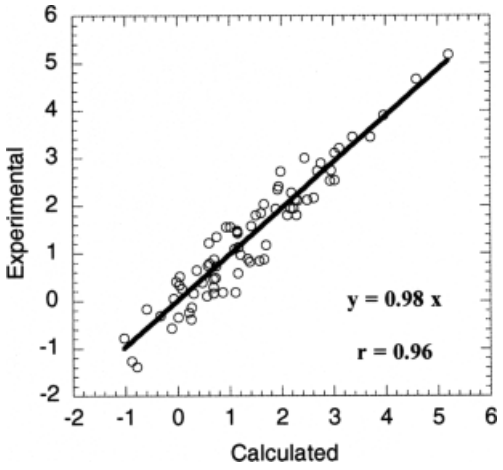


**FIGURE 3.** Representation of the octanol/water partition coefficient determined from the MST–HF/6-31G(d) free energies of solvation in water and octanol.

expensive. However, as noted in the Introduction, the availability of SCRF methods based on first-principles quantum mechanical calculations is valuable for the study of chemical phenomena in octanol, as well as to examine the transferability of fragment partition contributions. Thus, ongoing applications of the present work in our lab deal with aspects such as partitioning of solvation or transfer (octanol/water) free energies, which allow us to investigate, for instance, the effect of vicinal groups on the hydrophilic/hydrophobic properties of specific chemical fragments.[48–50] Likewise, another area of interest is the definition of similarity indexes based on the solvation or partitioning properties of molecules, and how this index can be exploited for the study of pharmacological properties (i.e., absorption through membranes) or ligand binding to receptors. Finally, another potential application currently investigated in our lab is the exploitation of MST–HF/6-31G(d) results for the development of simplified methods able to explore exhaustively the conformational preferences of (bio)molecules in condensed phases and their implications in the evaluation of partition coefficients.

**TABLE VI.**
**Calculated and Experimental *n*-Octanol/Water Partition Coefficient for a Series of Heterocyclic Compounds.**

| Compound | Calc. | Expt.[a] |
|---|---|---|
| Pyridine | 0.4 | 0.7 |
| Thiophene | 2.3 | 1.8 |
| Furan | 1.7 | 1.3 |
| Imidazole | −0.7 | −0.1 |
| Isoxazole | 0.7 | 0.1 |
| Pyrimidine | 0.1 | −0.4 |
| Pyrrole | 1.1 | 0.8 |
| Adenine | −0.2 | −0.1 |
| Guanine | −2.1 | −1.0 |
| Cytosine | −2.4 | −1.7 (−2.4) |
| Thymine | −0.7 | −0.6 |
| Uracil | −1.3 | −1.1 |
| Methyladenine | 0.4 | 0.0 |
| Methyluracil | −0.8 | −1.2 |

[a] When more than one $\log P_{ow}$ value is available, the value recommended by Hansch and Leo[71] is indicated, and the rest of values are given in parenthesis.

**TABLE VII.**
**Calculated and Experimental *n*-Octanol/Water Partition Coefficient for a Series of Conformationally Restricted Drugs.**

| Compound | Calc. | Expt.[a] |
|---|---|---|
| Acetaminophen | 0.6 | 0.5 (0.3) |
| Allopurinol | −1.3 | −0.6 |
| Amantadine | 2.9 | 2.4 |
| Amphetamine | 3.0 | 1.8 [−0.9, 1.8] |
| Aspirin | 1.6 | 1.2 (−1.2, 1.1) |
| Bifonazole | 3.5 | 4.8 |
| Caffeine | 1.3 | −0.1 [−0.2, 0.0] |
| Carbamazepine | 2.2 | 2.5 |
| Clonidine | 2.6 | 1.6 [0.5, 1.6] |
| Diazepam | 3.4 | 3.0 [2.5, 3.0] |
| Estradiol | 4.5 | 4.0 (2.3) |
| Flufenamic acid | 4.1 | 5.3 (2.1) |
| Ibuprofen | 3.4 | 3.5 (1.1, 1.7, 4.5) |
| Indoprofen | 2.5 | 2.8 (−0.4, −0.2) |
| Ketoprofen | 2.8 | 3.1 (−0.3, 0.0) |
| Lorazepam | 2.9 | 2.4 (1.9) |
| Naproxen | 3.6 | 3.3 (0.3) |
| Nicotine | 2.4 | 1.2 (0.3, 0.5) |
| Nifuroxime | 1.4 | 0.3 |
| Oxazepam | 2.0 | 2.2 (2.0) |
| Phenacetin | 2.4 | 1.6 (1.1, 1.7) |
| Phenytoin | 2.5 | 2.5 (2.0) |
| Proxicromil | 5.4 | 4.4 (1.6, 1.7) |
| Salicylic acid | 1.4 | 2.3 [−0.9, 2.3] |
| Sucrose | −4.5 | −3.7 (−3.0) |
| Testosterone | 3.2 | 3.3 (2.7) |
| 5-Fluorouracil | −2.0 | −0.9 [−0.8, −1.0] |

[a] When more than one $\log P_{ow}$ value is available, the value recommended by Hansch and Leo[71] is chosen, and the rest of values are given in parenthesis. When many data are compiled, the range of values is indicated in square brackets.

## Acknowledgments

We are indebted to Prof. C. J. Cramer for very valuable comments to this work. We are grateful to Prof. J. Tomasi for providing us with his original code of the PCM model, which was modified by us to carry out the MST calculations, and Prof. W. L. Jorgensen for giving us a copy of the BOSS3.4 computer program. C.C. was supported by a fellowship from the Ministerio de Educación y Cultura, and the authors thank the Centre de Supercomputació de Catalunya for financial facilities.

## Supporting Information

Tables containing the predicted free energies of solvation in water, chloroform, and carbon tetrachloride, as well as its electrostatic, cavitation, and van der Waals components, and the corresponding experimental data. A figure showing the comparison of the dipole moment in solution vs. the gas-phase values for the compounds included in the parametrization data set of these solvents.

## References

1. Carrupt, P.; Testa, B.; Gaillard, P. In Reviews in Computational Chemistry; Lipkowitz, K. B.; Boyd, D., Eds.; Wiley-VCH: New York, 1997; p. 241, vol. 11.
2. Sangster, J. Octanol–Water Partition Coefficients: Fundamentals and Physical Chemistry; Wiley: Chichester, 1997.
3. Hansch, C.; Leo, A. Exploring QSAR Fundamentals and Applications in Chemistry and Biology; American Chemical Society: Washington, DC, 1995.
4. Martin, Y. C. Quantitative Drug Design: A Critical Introduction; Marcel Dekker: New York, 1978.
5. Pliska, V.; Testa, B.; van de Waterbeemd, H., Eds. Lipophilicity in Drug Action and Toxicology; VCH: Weinheim, 1996.
6. Ren, S.; Das, A.; Lien, E. J. J. Drug Target 1996, 4, 103.
7. Abraham, M. H.; Platts, J. A.; Hersey, A.; Leo, A. J.; Taft, R. W. J Pharm Sci 1999, 88, 670.
8. Shih, P.; Pedersen, L. G.; Gibbs, P. R.; Wolfenden, R. J Mol Biol 1988, 280, 421.
9. Young, R. C.; Mitchell, R. C.; Brown, T. H.; Ganellin, C. R.; Griffiths, R.; Jones, M.; Rana, K. K.; Saunders, D.; Smith, I. R.; Sore, N. E.; Wilhs, T. J. J Med Chem 1988, 31, 656.
10. Hansch, C.; Fujita, T. J Am Chem Soc 1964, 86, 1616.
11. Leo, A.; Hansch, C.; Elkins, D. Chem Rev 1971, 71, 525.
12. Hansch, C.; Leo, A. Substituent Constants for Correlation Analysis in Chemistry and Biology; Wiley: New York, 1979.
13. Rekker, R. F. The Hydrophocbic Fragmental Constant; Elsevier: Amsterdam, 1977.
14. Mannhold, R.; Dross, K. Quantum Struct Act Relat 1996, 15, 403.
15. Viswanadhan, V. N.; Ghose, A. K.; Chandra Singh, U.; Wendoloski, J. J. J Chem Inf Comput Sci 1999, 39, 405.
16. Kamlet, M. J.; Doherty, R. M.; Abraham, M. H.; Marcus, Y.; Taft, R. W. J Phys Chem 1988, 92, 5244.
17. Abraham, M. H.; Chadha, H. S.; Whiting, G. S.; Mitchell, R. C. J Pharm Sci 1994, 83, 1085.
18. Haeberlein, M.; Brinck, T. J Chem Soc Perkin Trans 1997, 2, 289.
19. Lide, D. R., Ed. CRC Handbook of Chemistry and Physics; CRC Press: Boca Raton, FL, 1999; 80th ed.
20. Bernazzani, L.; Cabani, S.; Conti, G.; Mollica, V. J Chem Soc Faraday Trans 1995, 91, 649.
21. Orozco, M.; Luque, F. J Chem Rev 2000, 100, 4187.
22. Cramer, C. J.; Truhlar, D. G. Chem Rev 1999, 99, 2161.
23. Tomasi, J.; Persico, M. Chem Rev 1994, 94, 2027.
24. Jorgensen, W. L. Acc Chem Res 1989, 22, 184.
25. Kollman, P. A. Chem Rev 1993, 93, 2395.
26. Computer Simulation in Biomolecular Systems. Theoretical and Experimental Applications; van Gunsteren, W. F.; Weiner, P. K.; Wilkinson, A. J., Eds.; Kluwer: Dordrecht, 1997; vol. 3.
27. DeBolt, S. E.; Kollman, P. A. J Am Chem Soc 1995, 117, 5316.
28. Fernandes de Oliveira, C. A.; Werneck Guimaraes, C. R.; Bicca de Alencastro, R. Int J Quantum Chem 2000, 80, 999.
29. Essex, J. W.; Reynolds, C. H.; Richards, W. G. J Am Chem Soc 1992, 114, 3634.
30. Ekslerowiez, J. E.; Miller, J. L.; Kollman, P. A. J Phys Chem B 1997, 101, 10971.
31. Best, S. A.; Merz, K. M., Jr.; Reynolds, C. H. J Phys Chem B 1999, 103, 714.
32. Duffy, E. M.; Jorgensen, W. L. J Am Chem Soc 2000, 122, 2878.
33. Jorgensen, W. L.; Duffy, E. M. Biorg Med Chem Lett 2000, 10, 1155.
34. Bonaccorsi, R.; Floris, F.; Tomasi, J. J Mol Liq 1990, 47, 25.
35. Giesen, D. J.; Hawkins, G. D.; Liotard, D. A.; Cramer, C. J.; Truhlar, D. G. Theor Chem Acc 1997, 98, 85.
36. Giesen, D. J.; Chambers, C. C.; Cramer, C. J.; Truhlar, D. G. J Phys Chem B 1997, 101, 2061.
37. Giesen, D. J.; Chambers, C. C.; Cramer, C. J.; Truhlar, D. G. J Phys Chem B 1997, 101, 5084.
38. Li, J.; Zhu, T.; Hawkins, G. D.; Winget, P.; Liotard, D. A.; Cramer, C. J.; Truhlar, D. G. Theor Chem Acc 1999, 103, 9.
39. Hawkins, G. D.; Cramer, C. J.; Truhlar, D. G. J Phys Chem B 1997, 101, 7147.
40. Klamt, A.; Jonas, V.; Buerger, T.; Lohrenz, J. C. W. J Phys Chem A 1998, 102, 5074.
41. Klamt, A. J Phys Chem 1995, 99, 2224.
42. Klamt, A.; Schüürmann, G. J Chem Soc Perkin Trans 1993, 2, 799.
43. Best, S. A.; Merz, K. M., Jr.; Reynolds, C. H. J Phys Chem B 1997, 101, 10479.
44. Bachs, M.; Luque, F. J.; Orozco, M. J Comput Chem 1994, 15, 446.
45. Cubero, E.; Orozco, M.; Luque, F. J. J Am Chem Soc 1998, 120, 4723.
46. Cubero, E.; Orozco, M.; Luque, F. J. J Org Chem 1998, 63, 2354.

47. Colominas, C.; Luque, F. J.; Orozco, M. J Am Chem Soc 1996, 118, 6811.
48. Luque, F. J.; Barril, X.; Orozco, M. J Comput-Aided Mol Design 1999, 13, 139.
49. Muñoz, J.; Barril, X.; Luque, F. J.; Gelpi, J. L.; Orozco, M. In Advances in Molecular Similarity; Mezey, P. G.; Carbó-Dorca, R., Eds.; Kluwer: Dordrecht, to appear.
50. Barril, X.; Muñoz, J.; Luque, F. J.; Orozco, M. Phys Chem Chem Phys 2000, 2, 4897.
51. Orozco, M.; Bachs, M.; Luque, F. J. J Comput Chem 1995, 16, 563.
52. Luque, F. J.; Zhang, Y.; Aleman, C.; Bachs, M.; Gao, J.; Orozco, M. J Phys Chem 1996, 100, 4269.
53. Luque, F. J.; Aleman, C.; Bachs, M.; Orozco, M. J Comput Chem 1996, 17, 806.
54. Miertus, S.; Tomasi, J. Chem Phys 1982, 65, 239.
55. Miertus, S.; Scrocco, E.; Tomasi, J. Chem Phys 1981, 55, 117.
56. Pierotti, R. A. Chem Rev 1976, 76, 717.
57. Claverie, P. In Intermolecular Interactions: From Diatomics to Biomolecules; Pullman, B., Ed.; Wiley: Chichester, 1978.
58. Colominas, C.; Luque, F. J.; Teixidó, J.; Orozco, M. Chem Phys 1999, 240, 253.
59. Pascual-Ahuir, J. L.; Silla, E.; Tomasi, J.; Bonaccorsi, R. J Comput Chem 1987, 8, 778.
60. Jorgensen, W. L.; Maxwell, D. S.; Tirado-Rives, J. J Am Chem Soc 1996, 118, 11225.
61. Jorgensen, W. L. BOSS, Version 4.2; Yale University: New Haven, CT, 1999.
62. Singh, U. C.; Kollman, P. A. J Comput Chem 1984, 5, 129.
63. Besler, B. H.; Merz, K. M.; Kollman, P. A. J Comput Chem 1990, 11, 431.
64. Ferenczy, G. G.; Reynolds, C. A.; Richards, W. G. J Comput Chem 1990, 11, 341.
65. Orozco, M.; Luque, F. J. J Comput Chem 1990, 11, 909.
66. Hariharan, P. C.; Pople, J. A. Theor Chim Acta 1973, 28, 213.
67. Cabani, S.; Conti, G.; Mollica, V.; Bernazzani, L. J Chem Soc Faraday Trans 1991, 87, 2433.
68. Berti, P.; Cabani, S.; Conti, G.; Mollica, V. J Chem Soc Faraday Trans 1986, 82, 2547.
69. Riebesehl, W.; Tomlinson, E. J Solut Chem 1986, 15, 141.
70. Dallas, A. J.; Carr, P. W. J Chem Soc Perkin Trans 1992, 2, 2155.
71. Hansch, C.; Leo, A. Exploring QSAR: Hydrophobic, Electronic and Steric Constants; American Chemical Society: Washington, DC, 1995.
72. Peterson, M.; Poirier, R. MonsterGauss; Department of Biochemistry, Univ. of Toronto, Canada. Version modified by Cammi, R.; Tomasi, J. (1987); and by Luque, F. J.; Orozco, M. (2000).
73. Frisch, M. J.; Trucks, G. W.; Schlegel, H. B.; Gill, P. M. W.; Johnson, B. G.; Robb, M. A.; Cheeseman, J. R.; Keith, T. A.; Petersson, G. A.; Montgomery, J. A.; Raghavachari, K.; Al-Laham, M. A.; Zakrzewski, V. G.; Ortiz, J. V.; Foresman, J. B.; Cioslowski, J.; Stefanov, B. B.; Nanayakkara, A.; Challacombe, M.; Peng, C. Y.; Ayala, P. Y.; Chen, W.; Wong, M. W.; Andres, J. L.; Replogle, E. S.; Gomperts, R.; Martin, R. L.; Fox, D. J.; Binkley, J. S.; Defrees, D. J.; Baker, J.; Stewart, J. P.; Head-Gordon, M.; Gonzalez, C.; Pople, J. A. Gaussian 94, Revision A.1; Gaussian Inc.: Pittsburgh, PA, 1995.
74. Gao, J.; Luque, F. J.; Orozco, M. J Chem Phys 1993, 98, 2975.
75. Orozco, M.; Luque, F. J.; Habibollahzadeh, D.; Gao, J. J Chem Phys 1995, 102, 6145.
76. Pollack, G. L.; Kenna, R. P.; Himm, J. F.; Carr, P. W. J Chem Phys 1989, 90, 6569.
77. Wilcock, R. J.; Battino, R.; Danforth, W. F.; Wilhelm, E. J Chem Thermodyn 1978, 10, 817.
78. Chambers, C. C.; Hawkins, G. D.; Cramer, C. J.; Truhlar, D. G. J Phys Chem 1996, 1000, 16385.
79. Barone, V.; Cossi, M.; Tomasi, J. J Chem Phys 1997, 107, 3210.
80. Conçalves, P. F. B.; Livotto, P. R. Chem Phys Lett 1999, 304, 438.
81. Aguilar, M. A.; Olivares del Valle, F. J Chem Phys 1989, 129, 439.
82. Stefanovich, B. V.; Truong, T. N. Chem Phys Lett 1995, 244, 65.
83. Rashin, A. A.; Namboodiri, K. J Phys Chem 1987, 91, 6003.